Short Communication | Open Access

Chemical Synthesis

Li *et al. Chem. Synth.* **2026**, *6*, 71 **DOI:**10.20517/cs.2026.22

Electrocatalytic CO reduction to multi-carbon alcohols on functional ionic liquid-incorporated Cu-based electrodes

Jiaran Li[1,#], Lingzhi Ding[1,#], Yushan Ma[2,#], Rongxing Qiu[3], Jinlong Wan[1], Xincun Tang[2], Haikun Xu[4], Shuliang Yang[1,*], Jun Li[1,*], Li Peng[1,*]

Keywords:
Electrocatalysis, ionic liquids, electrocatalytic CORR, nanocatalysts, green synthesis

Citation: Li, J.; Ding, L.; Ma, Y.; Qiu, R.; Wan, J.; Tang, X.; Xu, H.; Yang, S.; Li, J.; Peng, L. Electrocatalytic CO reduction to multi-carbon alcohols on functional ionic liquid-incorporated Cu-based electrodes. *Chem. Synth.* **2026**, *6*, 71. https://dx.doi.org/10.20517/cs.2026.22

Received: 28 Apr 2026
First Decision: 9 Jun 2026
Revised: 14 Jun 2026
Accepted: 24 Jun 2026
Published: 27 Aug 2026

Academic Editors:
Da-Gang Yu, Qinggong Zhu
Copy Editor:
Pei-Yun Wang
Production Editor:
Pei-Yun Wang

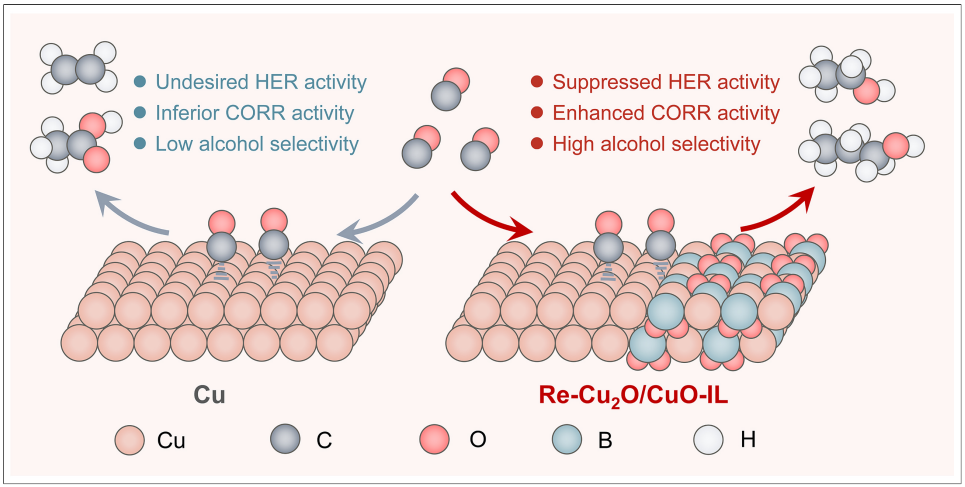

Abstract

Electrocatalytic reduction of CO_2/CO to multicarbon (C_{2+}) alcohols on copper-based catalysts often suffers from low selectivity, primarily arising from the rapid degradation of highly active Cu^+ sites and insufficient surface coverage of key reaction intermediates. Herein, we report a flower-like Cu_2O/CuO electrocatalyst modified with a multifunctional ionic liquid (IL), 1-octyl-3-methylimidazolium tetrafluoroborate ([Omim][BF_4]), to overcome these challenges. The $[Omim]^+$ cation of [Omim][BF_4] directs the formation of a hierarchical structure during the catalyst synthesis. Furthermore, the $[BF_4]^-$ anion serves as a boron source to promote the *in situ* generation of $CuBO_2$ under electrocatalytic reduction conditions, thereby effectively stabilizing the Cu^+ active species. Consequently, electrochemical evaluations reveal that Cu_2O/CuO-IL exhibits an encouraging Faradaic efficiency of 52.7% for C_{2+} alcohols ($FE_{ethanol}$: 25.6%, and $FE_{n\text{-}propanol}$: 27.1%) at -0.77 V *vs.*

[1]Department of Chemical and Biochemical Engineering, State Key Laboratory of Physical Chemistry of Solid Surface, College of Chemistry and Chemical Engineering, College of Energy, Xiamen University, Xiamen 361005, Fujian, China.
[2]College of Chemistry and Chemical Engineering, Central South University, Changsha 410083, Hunan, China.
[3]School of Optical and Electronic Information, Huazhong University of Science and Technology, Wuhan 430074, Hubei, China.
[4]Information and Network Center, Central South University, Changsha 410083, Hunan, China.
[#]These authors contributed equally.

***Correspondence to:** Prof. Li Peng, Prof. Shuliang Yang, Prof. Jun Li, Department of Chemical and Biochemical Engineering, State Key Laboratory of Physical Chemistry of Solid Surface, College of Chemistry and Chemical Engineering, College of Energy, Xiamen University, Xiamen 361005, Fujian, China. E-mail: li.peng@xmu.edu.cn; ysl@xmu.edu.cn; junnyxm@xmu.edu.cn

reversible hydrogen electrode (RHE). *In situ* Raman spectroscopy further corroborates the sustained Cu^+ retention and enhanced surface coverage of the pivotal *CO intermediate during the CO reduction reaction (CORR). This work demonstrates that a rational IL-directed surface engineering effectively stabilizes reactive Cu^+ species and advances the selective electrosynthesis of C_{2+} alcohols.

INTRODUCTION

Rising anthropogenic CO_2 emissions demand sustainable carbon conversion technologies[1]. While electrochemical CO_2 reduction reaction (CO_2RR) on copper (Cu)-based catalysts provides a promising pathway for synthesizing valuable multi-carbon (C_{2+}) products, its selectivity is hindered by unstable oxygenated intermediates and parasitic carbonate formation[2]. Alternatively, electrochemical CO reduction reaction (CORR) avoids CO_2 loss and suppresses C_1 products, yet directing high selectivity toward C_{2+} alcohols remains challenging[3]. Morphology engineering and surface modification have been explored to enhance product selectivity, with confined structures shown to increase *CO coverage and promote C–C coupling[4,5]. Moreover, Cu^+ species facilitate *CO dimerization but are intrinsically unstable and readily reduced to Cu^0 under reaction conditions[6]. Consequently, recent efforts, including heteroatom incorporation (e.g., iodine or boron) and functional molecular modification, have demonstrated that stabilizing Cu^+ species and tuning the local electronic structure are imperative for improving the selectivity toward C_{2+} alcohols[7,8].

Building on these insights, we report an ionic liquid (IL)-assisted strategy for the rational design of a flower-like Cu_2O/CuO-IL catalyst with enhanced selectivity toward C_{2+} alcohols. The imidazolium-based 1-octyl-3-methylimidazolium tetrafluoroborate ([Omim][BF_4]) exhibits dual functionality. Specifically, the $[Omim]^+$ cation directs the formation of hierarchical flower-like microspheres assembled by interconnected nanosheets, while the $[BF_4]^-$ anion acts as a boron source to generate $CuBO_2$ *in situ* during electroreduction. This bifunctional role effectively stabilizes the active Cu^+ species and enhances *CO coverage, thereby accelerating C–C coupling. Thus, the Cu_2O/CuO-IL catalyst achieves an impressive Faradaic efficiency of 52.7% for C_{2+} alcohols ($FE_{C2+\ alcohols}$) at -0.77 V *vs.* reversible hydrogen electrode (RHE) ($FE_{ethanol}$: 25.6%, and $FE_{n\text{-}propanol}$: 27.1%). This work provides a versatile approach to regulate catalyst reconstruction and preserve active sites by employing IL as structure-directing agent and a heteroatom source.

RESULTS AND DISCUSSION

A series of Cu-based catalysts were synthesized via a one-pot solvothermal method with varying [Omim][BF_4] concentration [Supplementary Figures 1 and 2]. Morphological characterization revealed an IL-concentration-dependent evolution from irregular pristine Cu nanoparticles to flower-like architectures composed of interconnected nanosheets at optimal IL loading [Figure 1A and B, Supplementary Figure 3]. This structural transformation was directed by the surfactant-like $[Omim]^+$ cation, which acted as soft template to construct hierarchical structures, thereby maximizing the active surface area and facilitating mass transport. The high-resolution transmission electron microscope (HRTEM) image of Cu_2O/CuO-IL clearly shows the Cu_2O(111) and CuO(002) facets [Figure 1C]. Powder X-ray diffraction (PXRD) analysis revealed that modulating the [Omim][BF_4] content (0-2.0 mol) drove a phase evolution from metallic Cu to Cu_2O, Cu_2O/CuO, and CuO, while simultaneously diminishing the overall crystallinity [Figure 1D]. Fourier transform infrared (FT-IR) spectra of the [Omim][BF_4]-modified catalysts exhibited characteristic C–H and B–F vibrations, indicating the successful IL incorporation [Figure 1E]. Thermal gravimetric analysis (TGA) curves quantified the grafting amounts of IL [Figure 1F and Supplementary Table 1]. X-ray photoelectron spectroscopy (XPS) revealed the coexisting Cu^+ and Cu^{2+} species in Cu_2O/CuO-IL [Figure 1G], consistent with the lattice fringes observed in the HRTEM image. Conversely, the bare Cu catalyst only possessed a

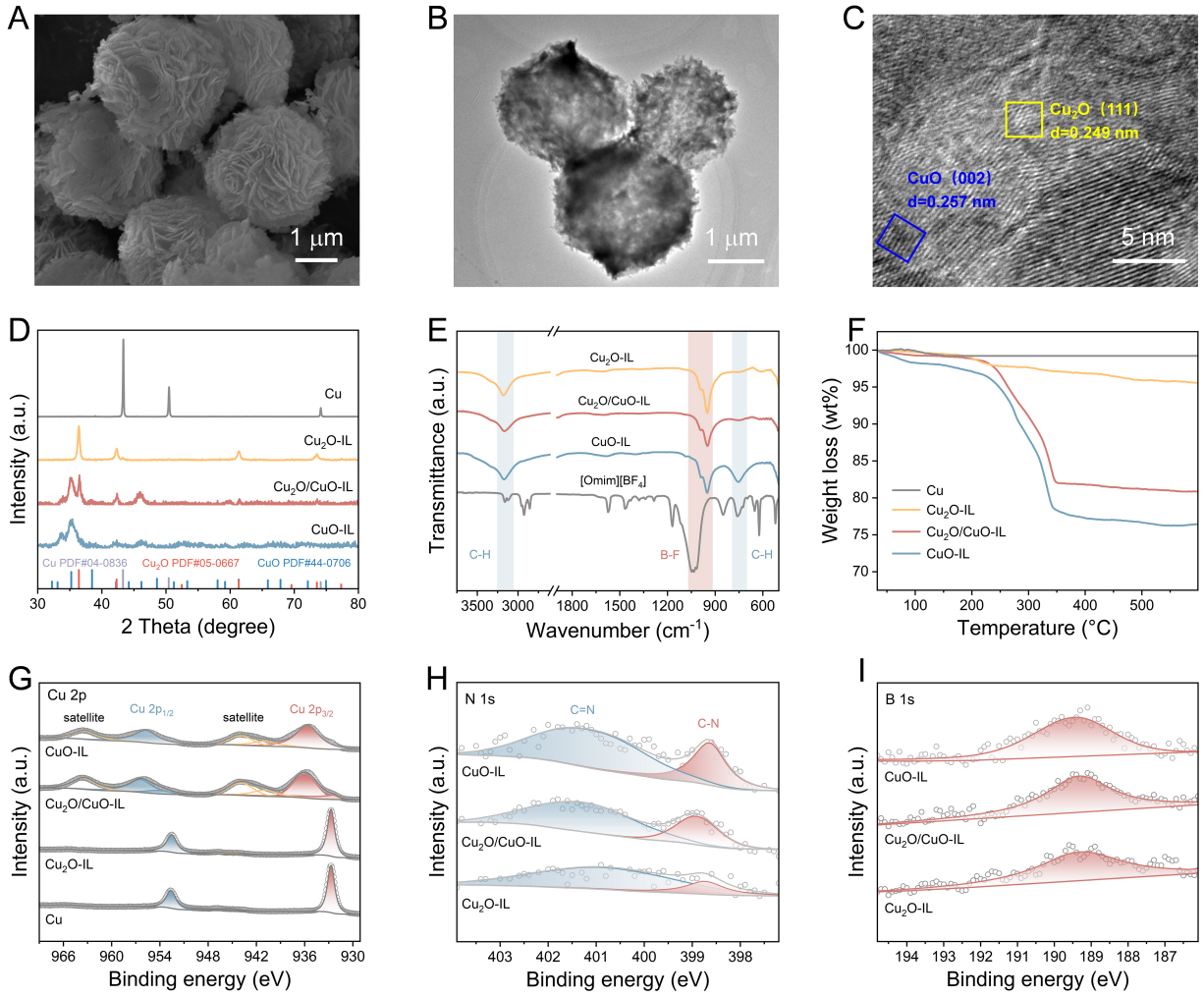

Figure 1. Structural characterization of IL-modified Cu-based catalyst. (A) SEM, (B) TEM, and (C) HRTEM images of Cu_2O/CuO-IL catalyst; (D) PXRD patterns of Cu-based catalysts with and without [Omim][BF_4] modification; (E) FT-IR spectra of [Omim][BF_4] and [Omim][BF_4]-modified Cu-based catalysts; (F) TGA curves; (G) Cu 2p, (H) N 1s, and (I) B 1s XPS spectra of Cu-based catalysts with and without [Omim][BF_4] modification. IL: Ionic liquid; SEM: scanning electron microscope; TEM: transmission electron microscope; HRTEM: high-resolution transmission electron microscope; PXRD: powder X-ray diffraction; [Omim][BF_4]: 1-octyl-3-methylimidazolium tetrafluoroborate; FT-IR: Fourier transform infrared; TGA: thermal gravimetric analysis; XPS: X-ray photoelectron spectroscopy.

metallic Cu^0 phase [Supplementary Figure 4]. Moreover, the presence of the imidazolium ring and B in [Omim][BF_4] was further supported by N 1s and B 1s spectra, respectively [Figure 1H and I]. Elemental mapping images demonstrated the homogeneous distribution of [Omim][BF_4] throughout the catalyst, indicating the uniform IL dispersion on Cu_2O/CuO-IL [Supplementary Figure 5]. These results collectively confirm the successful integration of [Omim][BF_4], which simultaneously modulates the surface microenvironment and electronic structure of the Cu-based catalysts.

The CORR performance of both pristine and IL-modified Cu-based catalysts was then systematically evaluated in a flow cell to determine the influence of the [Omim][BF_4] modifier [Supplementary Figure 6]. Compared with pristine Cu, [Omim][BF_4]-modified catalysts exhibited significantly enhanced current density and selectivity toward C_{2+} alcohols [Figure 2A-C]. Notably, the Cu_2O/CuO-IL catalyst achieved a maximum $FE_{C2+\ alcohol}$ of 52.7% at -0.77 V *vs.* RHE ($FE_{ethanol}$: 25.6% and $FE_{n\text{-}propanol}$: 27.1%), with a partial current density of ~52 mA·cm^{-2} [Figure 2B and C, Supplementary Figure 7]. In contrast, the pristine Cu showed negligible n-propanol production under identical conditions. The enhanced CORR performance was further

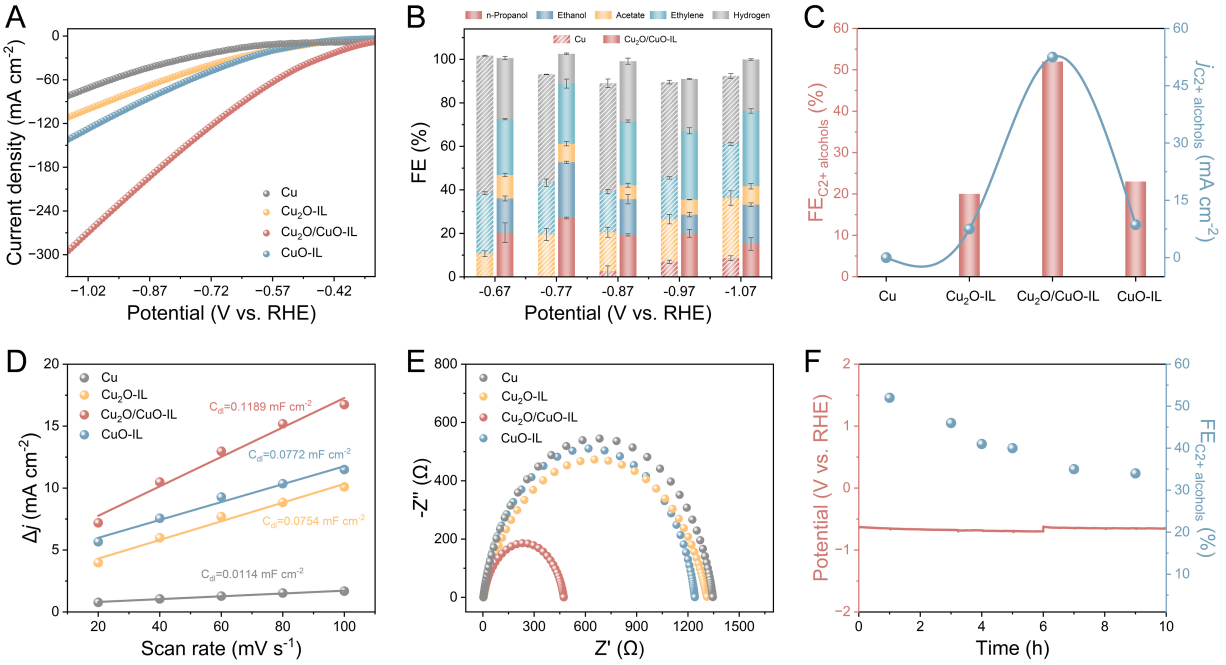

Figure 2. CO electroreduction performance. (A) Linear sweep voltammetry curves; (B) FEs of all CORR products at different potentials over pure Cu and Cu_2O/CuO-IL catalysts [Error bars represent SD from three independent replicates (n = 3 per group; rectangle filled with lines: Cu catalyst; solid-filled rectangle: Cu_2O/CuO-IL catalyst)]; (C) $FEs_{C2+\ alcohols}$ and partial current densities for C_{2+} alcohols; (D) C_{dl} plots; (E) Nyquist plots of Cu-based catalysts with and without IL modification; (F) Stability for CORR over the Cu_2O/CuO-IL catalyst. FEs: Faradaic efficiencies; CORR: CO reduction reaction; IL: ionic liquid; SD: standard deviation; RHE: reversible hydrogen electrode.

verified by comprehensive electrochemical measurements. [Omim][BF_4]-modified catalysts exhibited more positive onset potentials, lower charge-transfer resistance, and larger electrochemically active surface areas than pristine Cu, collectively reflecting improved intrinsic activity and greater accessibility of active sites [Figure 2D and E, Supplementary Figure 8]. Evaluation of the stability of Cu_2O/CuO-IL revealed that the $FE_{C2+\ alcohols}$ remained above 30% over 10 h of continuous operation [Figure 2F]. These results clearly demonstrate that the introduction of [Omim][BF_4] on Cu-based catalysts enables efficient C_{2+} alcohol production.

Structural characterization was further performed on the post-reaction catalysts to elucidate the reasons driving the product distributions. PXRD pattern, XPS spectrum, and HRTEM image revealed that Cu_2O/CuO-IL underwent pronounced electrochemical reconstruction to form small Cu/$CuBO_2$ particles [Figure 3A and B, Supplementary Figures 9 and 10]. Furthermore, the XPS spectrum presented a noticeable negative shift in B 1s binding energy after electrolysis, attributed to the weaker electron-withdrawing property of O in $CuBO_2$ compared with F in [Omim][BF_4] [Figure 3C]. This structural transformation originated from the hydrolysis of $[BF_4]^-$ and the subsequent reaction with Cu^+ species to form $CuBO_2$.

To clarify the enhanced C_{2+} alcohol selectivity on [Omim][BF_4]-modified Cu catalyst, *in situ* Raman spectroscopy was employed to detect the active species on the catalyst surface during CORR. Both Cu and Cu_2O/CuO-IL exhibited characteristic bands at ~293 and 2,120 cm^{-1}, assigned to the Cu–CO and C≡O stretching vibrations of atop-bound *CO intermediate ($*CO_{atop}$)[9,10], respectively [Figure 3D and E]. The substantially higher peak intensities for Cu_2O/CuO-IL than the bare Cu indicate an elevated *CO surface coverage, driven by the intermediate confinement effect of the imidazolium alkyl chains. Furthermore, time-resolved Raman spectra of Cu_2O/CuO-IL presented progressively intensified peaks at 220 and 499 cm^{-1}, corresponding to active Cu^+ species and Cu–O–B bonds[11,12], respectively [Figure 3F]. These observations

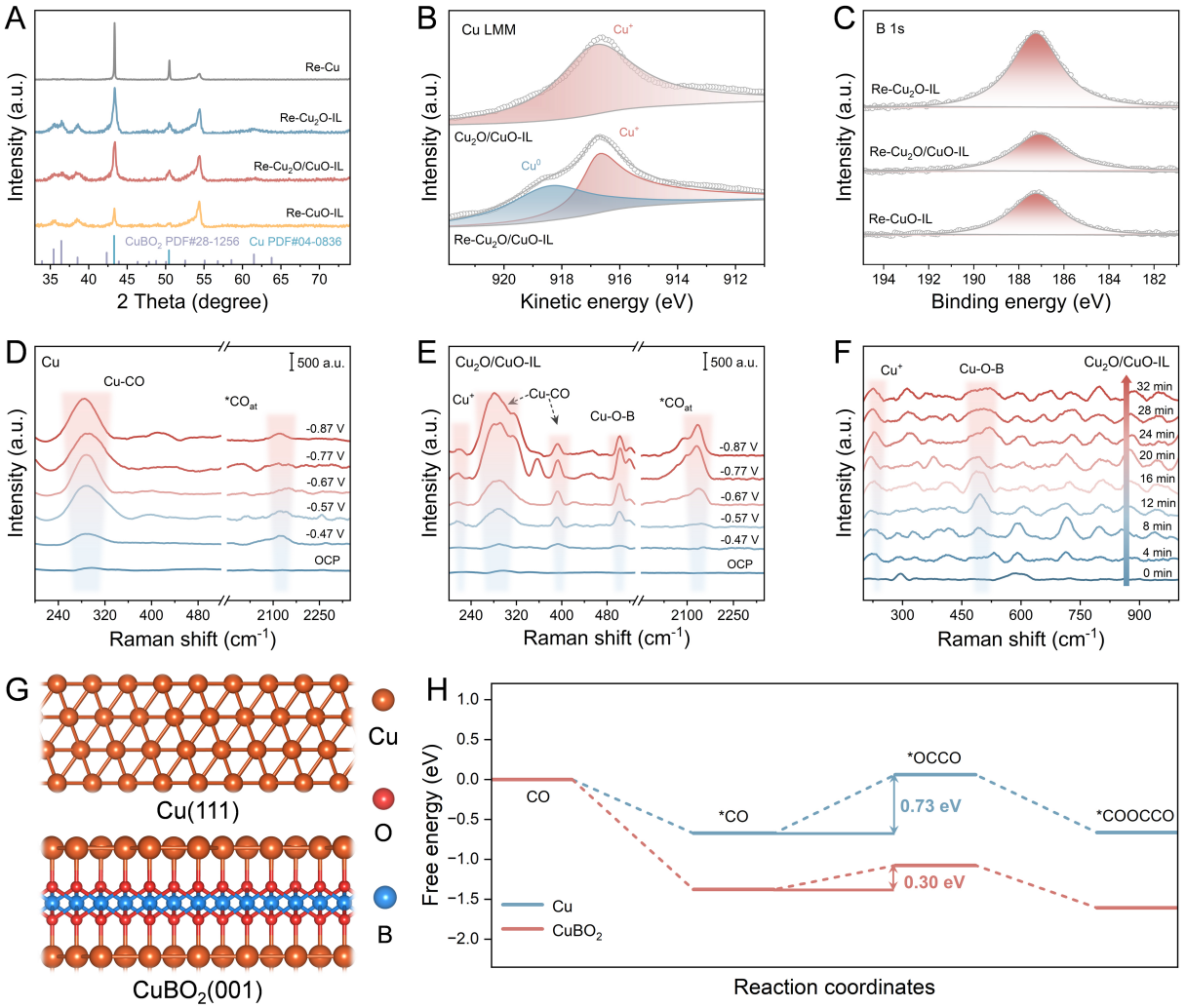

Figure 3. Investigation of reaction mechanism. (A) PXRD patterns of Cu-based catalysts with and without IL modification after CORR; (B) Comparison of Cu LMM spectra of Cu_2O/CuO-IL before and after CORR; (C) Comparison of B 1s spectra of IL-modified Cu-based catalysts after CORR; *In situ* Raman spectra of (D) Cu and (E) Cu_2O/CuO-IL during CORR at various potentials; (F) Time-resolved *in situ* Raman spectra of Cu_2O/CuO-IL during CORR; (G) Optimized models of Cu(111) and $CuBO_2$(001); (H) Reaction free energies for the formation of C_{2+} alcohols on Cu and $CuBO_2$. PXRD: Powder X-ray diffraction; IL: ionic liquid; CORR: CO reduction reaction; LMM: one type of Auger electron peak; OCP: open circuit potential.

demonstrate that B retains oxygen to stabilize Cu^+ active sites. Consequently, the synergy of elevated *CO coverage and robust Cu^+ stabilization explains the superior C_{2+} alcohol generation on Cu_2O/CuO-IL compared to bare Cu.

Density functional theory (DFT) calculations on $CuBO_2$(001) and Cu(111) models further elucidate the enhanced C_{2+} alcohol selectivity of IL-derived $CuBO_2$ during CORR [Figure 3G]. *CO adsorption is thermodynamically favored on $CuBO_2$ (-1.38 eV) compared to bare Cu (-0.67 eV). This enhanced affinity originates from electron-deficient B atoms (empty p-orbitals) that suppress lattice oxygen loss and electronically stabilize Cu^+ active sites, directly corroborating *in situ* Raman observations [Figure 3H, Supplementary Figures 11 and 12]. Furthermore, the barrier for the rate-determining *CO dimerization (*OCCO formation) on $CuBO_2$ is merely 0.30 eV, substantially lower than on Cu (0.73 eV). By simultaneously elevating local *CO coverage and kinetically facilitating C–C coupling, the B-modulated Cu^+ species seamlessly overcome the C_2 formation bottleneck. This drives subsequent hydrogenation to ethanol

or $*C_2$–$*C_1$ coupling toward n-propanol, whereas the weak *CO affinity and high coupling barrier on bare Cu severely hinder C_{2+} alcohol synthesis.

CONCLUSION

In summary, we report a one-pot method to synthesize the flower-like Cu-based nanocatalysts utilizing [Omim][BF_4] as a versatile modifier. The Cu_2O/CuO-IL catalyst with the optimal IL content achieves a $FE_{C2+\ alcohols}$ of 52.7% at -0.77 V *vs.* RHE (including $FE_{ethanol}$ of 25.6% and $FE_{n\text{-}propanol}$ of 27.1%), which is superior to the pristine Cu catalyst. Structure characterization and *in-situ* Raman results confirm that IL modification stabilizes the active Cu^+ species and enhances the *CO coverage, facilitating selective generation of C_{2+} alcohols. This work not only provides valuable guidance for elucidating the formation mechanism of high-value-added C_{2+} alcohols, but also offers a strategy for designing high-performance catalysts via IL surface modification in accordance with green chemistry principles.

DECLARATIONS

Authors' contributions

Supervised the project and revised the manuscript: Peng, L.; Yang, S.; Li, J. (Jun Li)
Performed the experiments, data analysis, and wrote the original manuscript: Li, J. (Jiaran Li); Ding, L.; Qiu, R.; Wan, J.
Conducted the theoretical calculations: Ma, Y.; Tang, X.; Xu, H.

Availability of data and materials

The data supporting the findings of this study are available within this article and its Supplementary Materials. Further data are available from the corresponding authors upon reasonable request.

AI and AI-assisted tools statement

Not applicable.

Financial support and sponsorship

This work was supported by the National Natural Science Foundation of China (No. 22373080; 22078274), the Fujian Provincial Natural Science Foundation of China (No. 2024J08008), the Fundamental Research Funds for the Central Universities (No. 20720240054), and the Nan-qiang Youth Scholar Program of Xiamen University and Xiaomi Young Talents Program/Xiaomi Foundation.

Conflicts of interest

All authors declared that there are no conflicts of interest.

Ethical approval and consent to participate

Not applicable.

Consent for publication

Not applicable.

Supplementary Materials

Supplementary Materials

REFERENCES

1. Zheng, L.; Fang, C.; Chen, Z.; et al. Advancing CO_2 conversion: integrated use of dual active catalytic sites in flexible, porous polymeric porphyrin and ionic liquid composite networks. *Chem. Synth.* **2026**, *6*, 12. DOI
2. Qiu, R.; Li, J.; Du, J.; et al. Promoting acetate production on the in situ reconstructed Cu nanoislands via pressure-regulated CO adsorption and electroreduction. *Sci. Bull.* **2025**, *70*, 3794-802. DOI PubMed

3. Kim, J. Y. T.; Sellers, C.; Hao, S.; Senftle, T. P.; Wang, H. Different distributions of multi-carbon products in CO_2 and CO electroreduction under practical reaction conditions. *Nat. Catal.* **2023**, *6*, 1115-24. DOI
4. Liu, J.; You, F.; He, B.; et al. Directing the architecture of surface-clean Cu_2O for CO electroreduction. *J. Am. Chem. Soc.* **2022**, *144*, 12410-20. DOI PubMed
5. Soodi, S.; Zhang, J. J.; Zhang, J.; et al. Selective electroreduction of CO_2 to C_{2+} products on cobalt decorated copper catalysts. *Chem. Synth.* **2024**, *4*, 44. DOI
6. Fan, Y.; Yan, Y.; Xia, Z.; et al. Halide-induced Cu^+ sites for efficient CO electroreduction to n-propanol. *Chem. Catal.* **2026**, *6*, 101688. DOI
7. Shen, Y.; Fang, N.; Liu, X.; et al. Observation of metal-organic interphase in Cu-based electrochemical CO_2-to-ethanol conversion. *Nat. Commun.* **2025**, *16*, 2073. DOI PubMed
8. Zhou, Y.; Che, F.; Liu, M.; et al. Dopant-induced electron localization drives CO_2 reduction to C_2 hydrocarbons. *Nat. Chem.* **2018**, *10*, 974-80. DOI
9. Chen, X.; Chen, J.; Alghoraibi, N. M.; et al. Electrochemical CO_2-to-ethylene conversion on polyamine-incorporated Cu electrodes. *Nat. Catal.* **2021**, *4*, 20-7. DOI
10. Zhang, R.; Zhang, J.; Wang, S.; et al. Synthesis of n-propanol from CO_2 electroreduction on bicontinuous Cu_2O/Cu Nanodomains. *Angew. Chem. Int. Ed. Engl.* **2024**, *63*, e202405733. DOI PubMed
11. Yu, F.; Shu, M.; Zhang, G.; Yu, Q.; Wang, H. Enhancing CO_2 electroreduction precision to ethylene and ethanol: the role of additional boron catalytic sites in Cu-based tandem catalysts. *Adv. Sci.* **2024**, *11*, e2410118. DOI PubMed PMC
12. Zhao, Y.; Chang, X.; Malkani, A. S.; et al. Speciation of Cu surfaces during the electrochemical CO reduction reaction. *J. Am. Chem. Soc.* **2020**, *142*, 9735-43. DOI PubMed